J Mater Sci: Mater Med (2011) 22:389–396
DOI 10.1007/s10856-010-4211-5

Seeding density matters: extensive intercellular contact masks the surface dependence of endothelial cell–biomaterial interactions

Yun Xia · Melissa Prawirasatya · Boon Chin Heng · Freddy Boey · Subbu S. Venkatraman

Received: 23 August 2010 / Accepted: 8 December 2010 / Published online: 8 January 2011

Abstract The effects of seeding density have often been overlooked in evaluating endothelial cell-biomaterial interactions. This study compared the cell attachment and proliferation characteristics of endothelial cells on modified poly (L-lactic acid) (PLLA) films conjugated to gelatin and chitosan at low and high seeding densities (5,000 and 50,000 cells/cm^2). During the early stage (2 h) of cell-biomaterial interaction, a low seeding density enabled us to observe the intrinsic surface-dependent differences in cell attachment capacity and morphogenesis, whereas extensive intercellular interactions at high seeding density masked differences between substrates and improved cell attachment on low-affinity substrates. During the later stage of cell-biomaterial interaction over 7-days of culture, the proliferation rate was found to be surface-dependent at low seeding density, whereas this surface-dependent difference was not apparent at high seeding density. It is recommended that low seeding density should be utilized for evaluating biomaterial applications where EC density is likely to be low, such as in situ endothelialization of blood-contacting devices.

1 Introduction

Rapid endothelialization is crucial for cardiovascular stents and grafts to prevent post-implantation thrombosis and restenosis [1]. With increasing demand for biodegradable stents/grafts [2], complete endothelialization has become even more crucial to prevent degradation debris from entering the bloodstream and causing adverse complications. In order to promote such endothelialization, substantial effort has been focused on suitably functionalizing the surfaces of biomaterial. For example, extracellular matrix (ECM) proteins (e.g. collagen, fibronectin and laminin) and functional domains of ECM components (e.g. RGD, YIGSR and REDV), have been immobilized on biomaterial surfaces [3, 4].

A wide range of cell seeding densities from 4×10^3 to 2×10^5 cells/cm^2 have been used for in vitro studies on endothelial cell-biomaterial interaction [5–12]. To date, there has been no established standard protocol to define the seeding density, which makes it difficult to compare different studies done on the same substrate. The biocompatibility of certain materials and protocols evaluated using relatively high seeding densities, might not be appropriate for applications whereby the availability of cells is limited. For example, in the case of in situ endothelialization of blood-contacting devices, regrowth of the endothelial layer might be derived from the migration of ECs from adjacent tissue ("trans-mural endothelialization") and/or attachment and proliferation or the circulating endothelial cell precursors [13–15]. Available cell density in both situations is considered to be low [16, 17].

It has long been recognized that cell-matrix adhesion is predominantly mediated by integrins, and adherent cells can sense their immediate environment through integrin-based adhesion complexes, namely focal adhesions (FA), tightly associated with the actin cytoskeleton [18]. Cell–cell adhesions are also sites of physical connection as well as signaling transduction structures for regulating cell behavior [19]. Cadherin is a key cell–cell adhesion molecule localized at adherens junctions [20] which has a

Y. Xia · M. Prawirasatya · B. C. Heng · F. Boey · S. S. Venkatraman (✉)
School of Materials Science and Engineering, Nanyang Technological University, 50 Nanyang Avenue, Nanyang 639798, Singapore
e-mail: assubbu@ntu.edu.sg

function similar to that of integrin, which may be considered its counterpart in the FA complex. Integrins and cadherins are two distinct families of transmembrane cell adhesion receptors. While integrins allow cells to adhere to the extracellular matrix, cadherins bind homotypically to cadherins on neighboring cells and are responsible for the development of adherens junctions in epithelial tissues. Arthur et al. [21] showed that the signaling cascades of both cell–matrix and cell–cell adhesion, transmitted through integrins and cadherins respectively, involve Rho proteins, which are key regulators in reorganization of the actin cytoskeleton. Other studies have demonstrated cross-talk between cell-matrix and cell–cell junctions and both types of junctions cooperatively regulate cell movement, proliferation, adhesion and polarization [22–24].

Stimuli from neighboring cells via interaction of cell-surface receptors and secreted growth factors/cytokines are strongly dependent on the cell density. When the cell density is low, direct cell–cell contacts are limited and cell-biomaterial interaction is expected to be pre-dominantly influenced by cell-substrate contact. As cell density increases, cell–cell interaction becomes more extensive and is expected to profoundly influence cellular responses to biomaterials [25]. This study reports on the evaluation of the effects of initial seeding density on the EC-biomaterial interaction, by comparing a low seeding density of 5,000 cells/cm^2 versus a high seeding density of 50,000 cells/cm^2 using human umbilical vein endothelial cells (HUVECs). Three different PLLA substrates, namely unmodified PLLA, PLLA–gAA–gelatin and PLLA–gAA–chitosan, were prepared as described previously [26]. During the early phase of EC-biomaterial interaction, cell attachment and morphogenesis are the main cellular responses, whereas cell proliferation is the main cellular response during the later phase.

2 Materials and methods

2.1 Surface modification and characterization of PLLA

PLLA (Purac Far East, Singapore) substrates were prepared as described previously [26]. Briefly, acrylic acids (AA, Sigma-Aldrich) were graft polymerized on argon-plasma treated PLLA surface. Gelatin (Type A, Sigma-Aldrich) and chitosan (Sigma-Aldrich) were then immobilized through covalent bond formation between carboxylic groups found on AA and amine groups found on gelatin or chitosan in water soluble carbodiimide. PLLA–gAA–gelatin and PLLA–gAA–chitosan refer to PLLA films modified with gelatin and chitosan respectively. Surface chemical composition and wettability were characterized by X-ray Spectrometer and contact angle respectively [26].

2.2 Cell attachment and proliferation

HUVECs (Lonza) were cultured in endothelial growth medium (EGM, Lonza) under 95% humidified atmosphere and 5% CO_2 at 37°C. Cells were dissociated with 0.025% trypsin–EDTA (Lonza) and washed in Dulbecco's modified eagle medium (DMEM, Gibco) for 3 min by centrifugation to avoid any interference associated with adhesive proteins from serum, and then seeded on the various PLLA substrates in DMEM at either a low seeding density of 5,000 cells/cm^2 whereby cells are sparsely distributed on the substrate, or a high seeding density of 50,000 cells/cm^2 which is comparable to cell density at confluence. After 2 h incubation, unattached cells were gently rinsed off. The number of attached cells was quantified by the WST-8 assay (Dojindo, Japan). Cell attachment percentage was quantified as $N_{2h}/N_{seeding} \times 100\%$, where N_{2h} and $N_{seeding}$ were the cell count at 2 h and the initial seeding respectively. The cell count in each experimental condition was monitored on alternate days until confluence was reached. Cell doubling time of an exponential proliferation was calculated according to the method as described previously [26].

2.3 Mechanistic study on improved cell attachment in high-density seeding

Two mechanisms are possible for the improvement of cell attachment at high-density seeding. The secreted growth factors and cytokines by HUVECs at high-density seeding are more concentrated than that at low-density seeding. In order to study the influence of secreted growth factors and cytokines on cell attachment, HUVECs of 5,000 cells/cm^2 were seeded on pristine PLLA substrates in both fresh and conditioned medium for comparison. Conditioned medium here was prepared by incubating fresh EGM with confluent HUVECs in a tissue culture flask for 24 h, and then collected to centrifugation (3,600 rpm, 10 min) so as to remove detached cells and debris. HUVECs were allowed to attach for 2 h. The cell attachment percentage was studied using WST-8 assay as described earlier.

It is also hypothesized that extensive cell–cell interaction between neighboring cells at higher density promotes cell attachment. In order to evaluate this hypothesis, HUVECs were seeded at a density of 5,000 cells/cm^2 on both pristine and pre-seeded PLLA. Pre-seeded PLLA here was prepared by incubating HUVECs on PLLA substrates at a density of 25,000 cells/cm^2 for 24 h. Cells were allowed to attach for 2 h, and the number of attached cells was quantified by the WST-8 assay as described earlier. The cell attachment percentage on bare PLLA was calculated as $N_{2h}/5000 \times 100\%$, where N_{2h} was the cell density after 2 h incubation. The cell attachment percentage on pre-seeded PLLA was calculated as $(N_{2h}-N_{pre})/5000 \times 100\%$, where N_{2h} and N_{pre}

were the cell density after 2 h incubation and the cell density of pre-seeding HUVECs respectively. All experiments were carried out in 24-well tissue culture plate.

2.4 Immunofluorescence analysis

Cells were fixed with 4% paraformaldehyde for 15 min, permeabilized with 0.1% Triton X-100 for 10 min, and incubated with 10% goat serum (DAKO) in PBS for 30 min at room temperature. Vinculin was labeled with mouse anti-human vinculin antibody (clone h Vin-1, Sigma-Aldrich) and visualized with goat anti-mouse IgG-FITC conjugate (Sigma-Aldrich). Actin filaments and nuclei were labeled with Alexa Fluor® 568 (Molecular Probe) and DAPI (Molecular Probe) respectively. Cell images were captured with an Olympus IX71 inverted fluorescent microscope and Leica TCS SP5 laser-scanning spectral confocal microscope (CLSM). Cell morphometric parameters, spreading area and aspect ratio, were analyzed by the Image Pro Plus software using a modified method of Treiser et al.[27].

2.5 Statistical analysis

Three experimental replicates ($n = 3$) were utilized in the cell attachment and proliferation study. The results are presented as mean ± SD. The cell spreading area and aspect ratio were plotted as box plots to show the data distribution and significant differences between measured groups. At least 50 cells were analyzed for each experimental group. Each box encompasses 25–75 percentiles, with extending-lines covering the 95th and 5th percentiles, the thin line representing the median (50th percentile), and the thick line representing the mean values. Values outside the 95th and 5th percentiles were treated as outliers, and are represented by diamond dots. Density-dependent cellular responses were analyzed using Student's *t*-test. Surface-dependent cellular responses were analyzed using analysis of variance (ANOVA). A *P* value of less than 0.05 was used to infer statistical significance of differences.

3 Results and discussions

3.1 Extensive intercellular contact masks the surface dependence of cell attachment

Cell attachment percentage values were compared between low and high seeding density experimental groups, with the results illustrated in Fig. 1a. In the case of 5,000 cells/cm^2 seeding density, the cell attachment percentage appeared to be surface dependent (ANOVA, $^*P < 0.05$). After 2 h incubation, about 30% of seeded cells had adhered on unmodified PLLA. The presence of immobilized

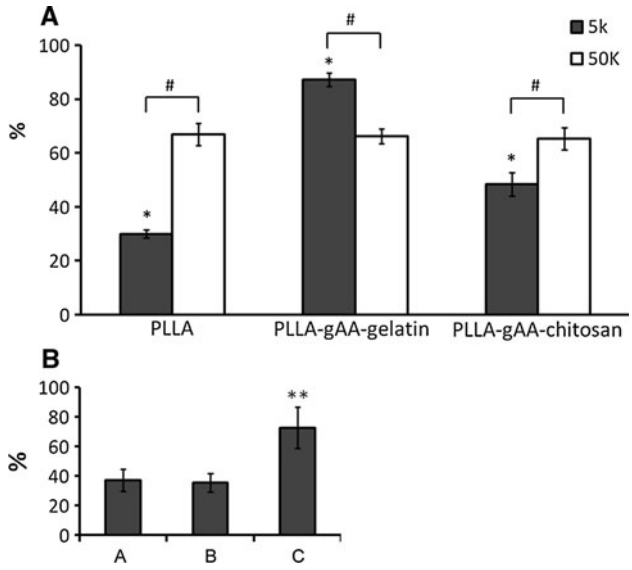

Fig. 1 **a** Extensive intercellular contact masks the surface dependence of cell adhesion. Surface-dependent cell adhesion was analyzed with ANOVA, $^*P < 0.05$. Density-dependent cell adhesion was analyzed with paired Student's *t*-test, $^\#P < 0.05$. **b** Growth factors and cytokines secretion showed no significant effect on cell attachment by comparing seeding in fresh medium (*A*) with that in conditioned medium (*B*). Pre-seeded cells on PLLA greatly promoted cell attachment ($^{**}P < 0.05$) by comparing seeding HUVEC on bare PLLA (*A*) with that on 25,000cell/cm^2 pre-seeded PLLA (*C*). After 2 h culture, unattached cells were removed by PBS rinsing. The number of remaining cells were measured by WST-8 reagent

biomolecules on the PLLA surface enhanced cell attachment: 90% attachment was observed on PLLA–gAA–gelatin and 50% on PLLA–gAA–chitosan. These observations agreed well with our previous study [26]. In contrast, the surface dependence of cell attachment was not observed at high seeding density of 50,000 cells/cm^2. Instead, all substrates appeared to be equivalent: about 70% of seeded cells were able to attach on all three PLLA substrates regardless of their differences in surface properties. High seeding density significantly improved cell attachment on PLLA and PLLA–gAA–chitosan ($^\#P < 0.05$). Interestingly, cell attachment percentage on PLLA–gAA–gelatin decreased from 90 to 70%. However, the total cell count on PLLA–gAA–gelatin in fact increased from 4,500 to 35,000. It is conceivable that high seeding density enhanced cell attachment during the early phase of cell-biomaterial interaction and masked any differences in the substrate surface. Surface dependence of cell attachment was only observed at low seeding density by eliminating intensive cell–cell interaction.

The improvement of cell attachment at high seeding density can possibly arise from two mechanisms: (a) In comparison to the low seeding density, the concentration of secreted growth factors and cytokines at high seeding density is higher, which could contribute to stronger cell

attachment signaling stimulation; (b) In comparison to the low seeding density, cell–cell interaction at high seeding density is more extensive, which could contribute to cell attachment signaling activation through crosstalk between cell-substrate and cell–cell adhesion.

To investigate the first possible mechanism, conditioned medium which is the EGM incubated with HUVECs for 24 h was used to represent the medium at high density seeding. Cell attachment on PLLA at 5,000 cells/cm^2 in conditioned medium was compared with that in fresh medium. As illustrated in Fig. 1b, cell attachment percentage values were about 37% in both conditions. This implies that increased secretion of growth factors and cytokines at high seeding densities had negligible effect on cell attachment during 2 h incubation.

To investigate the second possible mechanism, cell attachment on PLLA at 5,000 cells/cm^2 was compared with that on pre-seeded PLLA. As shown in Fig. 1b, a significant increase of cell attachment percentage from 37 to 72% was observed by pre-seeding PLLA. This strongly suggested that the presence of pre-seeded HUVEC promoted the attachment of incoming cells. This simple test demonstrated a possible scenario occurring at high seeding density, whereby adherent cells hastened the attachment of cells from free suspension, through cell–cell interaction followed by triggered cell-substrate attachment. Another possible scenario is that high seeding density favors the formation of cell–cell adhesion in suspension even prior to cell-substrate attachment. Clumps of associated cells sediment and attach on the substrate simultaneously, such that cell attachment was significantly improved even on low cell affinity substrates. At present, we cannot distinguish between these two possible mechanisms.

Zhu et al. [28, 29] showed that cell attachment on gelatin- and chitosan- modified PLLA (modified through aminolysis) was comparable at a seeding density of 12 × 10^4 cell/cm^2, which agrees with our results at high seeding density. However, our study demonstrated the superiority of cell attachment on PLLA–gAA–gelatin compared to PLLA–gAA–chitosan at a relatively low seeding density of 5,000 cell/cm^2. The data showed clearly that differences among substrates are more pronounced at low seeding density, but was masked at high seeding density. This should be taken into consideration whenever biomaterials are to be evaluated for use in applications involving low cell densities.

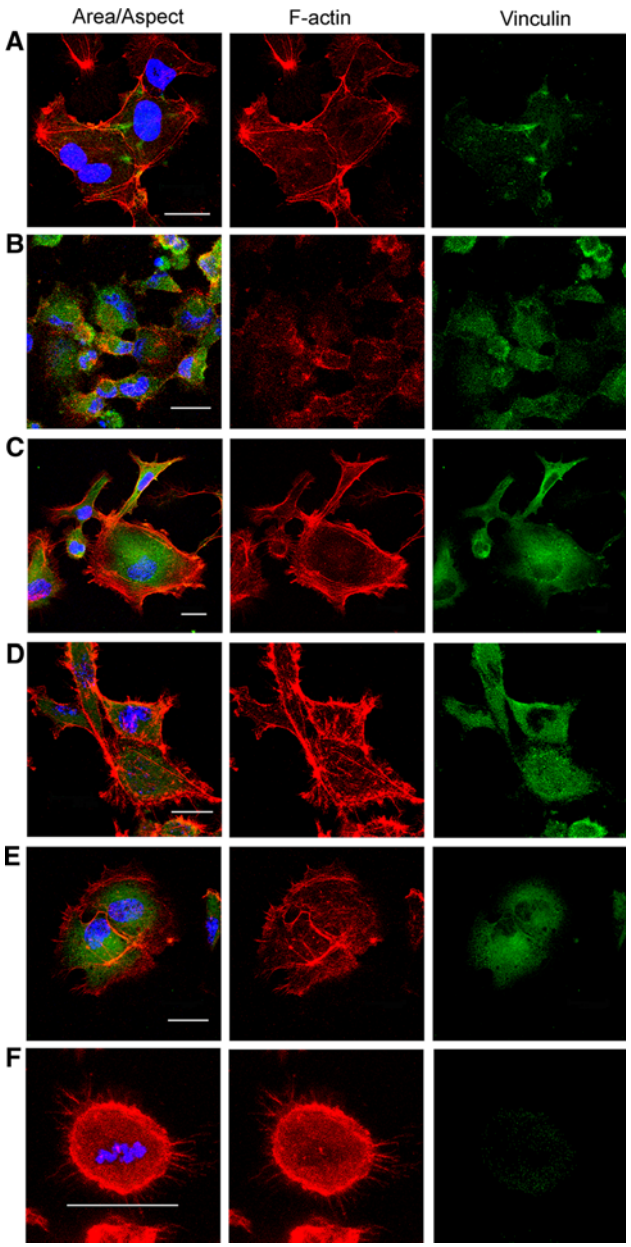

Fig. 2 Surface chemistry, rather than seeding density, influences cell morphogenesis. HUVECs were seeded on PLLA (*A* and *B*), PLLA–gAA–gelatin (*C* and *D*), and PLLA–gAA–chitosan (*E* and *F*) at low seeding density of 5000/cm^2 (*A*, *C* and *E*) or high seeding density of 50,000/cm^2 (*B*, *D* and *F*). After 2 h culture, unattached cells were removed by PBS rinsing. The remaining cells were fluorescently stained to label nuclei (DAPI), vinculin (FITC) and F-actin (Alexa Fluor® 568). The images were captured by Leica TCS SP5 CLSM. *Scale bar* 20 μm

3.2 Surface chemistry, rather than seeding density, influences cell morphogenesis

After 2 h incubation, cell morphology was observed with immunostaining of F-actin, vinculin and nuclei. As shown in Fig. 2, cell morphology did not exhibit distinctive differences upon comparing cells grown on the same substrate at low (5,000 cells/cm^2) and high (50,000 cells/cm^2) seeding densities. On PLLA–gAA–gelatin (Fig. 2c,d), cells observed at both seeding densities exhibited the characteristic morphology of spreading HUVEC. Bundles of F-actin were found in cell lamellipodia, which are the

broad, flat protrusions at the leading edge of a motile cell. Filopodia, the thin finger-like structures filled with tight parallel bundles of F-actin, were conspicuously protruding from the lamellipodia. Both of these are well-known structures involved in cell spreading and migration [30]. On PLLA–gAA–chitosan (Fig. 2e,f) seeded with either 5,000 or 50,000 cells/cm^2, the cells were observed to have significantly reduced spreading area in high-density seeding. This was further confirmed in the subsequent morphometric parameter analysis. Nevertheless, the typical spreading cell morphology was observed under both seeding density conditions, i.e. defined lamellipodia and filopodia with F-actin bundles localized mostly near the cell periphery. On PLLA (Fig. 2a,b), no obvious difference in cell morphology between low- and high-density seeding was found, other than the reduced cell spreading area. Compared with the cell morphology on gelatin- and chitosan-modified PLLA, much thinner F-actin bundles were observed beneath the cell membrane on bare PLLA and there was hardly any vinculin expression, thus indicating poor EC affinity for unmodified PLLA as demonstrated in our previous study [26].

Cell morphology was evaluated using two morphometric parameters, cell spreading area and aspect ratio. Cell spreading area measures the extent of cell spreading on a substrate as projection area. As shown in Fig. 3a, the cell spreading area observed from a confluent EC monolayer grown on tissue culture plate (TCPS) was 1,400 μm^2 on average. After 2 h incubation, cell spreading under any of the experimental conditions was not able to reach that value. It is also noted that cell spreading areas from the high seeding density group were significantly smaller than those observed in the low seeding density group. Spatial restriction is believed to be the main reason for the decrease in spreading area in the high seeding density group.

Normal EC displays a typical 'cobble-stone' morphology at confluence, with an epithelioid phenotype. By contrast, when cells are sparse or when intercellular junctions are disrupted, a fibroblastoid/mesenchymal morphology predominates. Cell aspect ratio is defined as the ratio of the major axis to the minor axis of an equivalent ellipse. In Fig. 3b, the cell aspect ratio of confluent EC monolayer grown on TCPS displaying cobble-stone morphology was about 2.38 on average.

Amongst the low-density seeding experimental group, the mean aspect ratio on PLLA–gAA–gelatin was about 2.80, suggesting a mesenchymal phenotype. By contrast, aspect ratios on PLLA and PLLA–gAA–chitosan were about 1.5, which were significantly less than that of cobble-stone morphology. This implied that although cells adhered on both surfaces, their cell morphology was somehow compromised. The absence of cell attachment ligands on

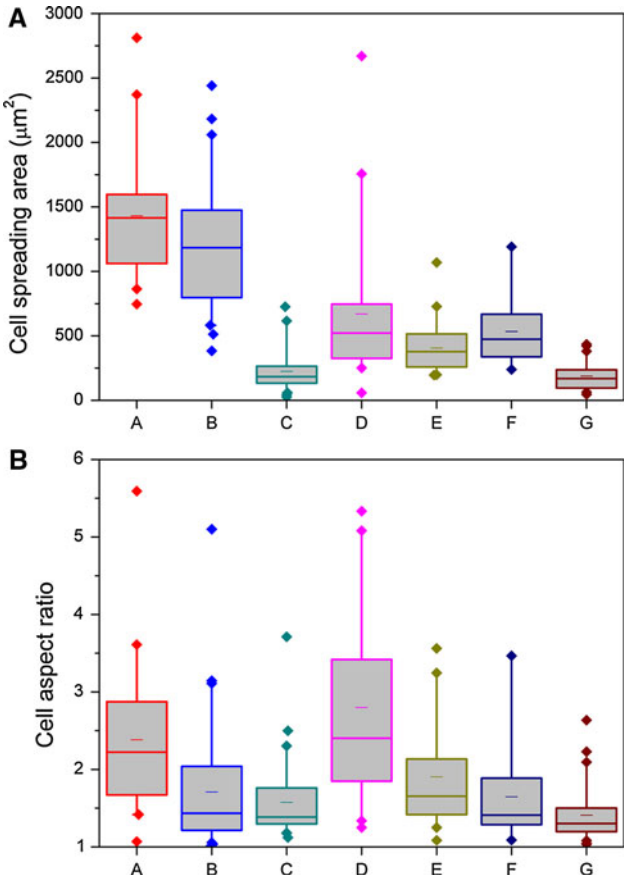

Fig. 3 Seeding density influenced **(a)** cell spreading area and **(b)** aspect ratio. Cell morphometric indicators observed on (*A*) TCPS, (*B* and *C*) PLLA, (*D* and *E*) PLLA–gAA–gelatin, (*F* and *G*) PLLA–gAA–chitosan. Cells on TCPS were confluent and incubated for 4 days. Low seeding density of 5000 cells/cm^2 was used on *B*, D, *F*. High seeding density of 50,000 cells/cm^2 was used on *C*, *E*, and *G*. High resolution immunofluorescent images of individual cells were taken by Leica TCS SP5 CLSM, and then analyzed by Image Pro Plus software. At least 50 cells were measured for each condition

PLLA and PLLA–gAA–chitosan is believed to be the main reason for the compromised cell morphology observed on both substrates. Unlike PLLA–gAA–gelatin, PLLA and PLLA–gAA–chitosan contained no cell attachment molecules/ligands on their surfaces. Cell attachment in serum-free medium relied largely on hydrophobic or electrostatic interaction between substrate and attachment ligands on the cell membrane. Amongst the high-density seeding experimental groups, cell aspect ratio on PLLA–gAA–gelatin was reduced to 1.90, mostly due to cell–cell contact inhibition. The cell aspect ratio on PLLA and PLLA–gAA–chitosan was similar to that at low-density seeding. It suggests that the dominant factor for aspect ratio is surface chemistry.

The data presented in Fig. 3 suggest that cell morphogenesis during the early stage of cell-biomaterial interaction was strongly dependent on substrate chemistry rather

than seeding density. However, seeding density did influence some cell morphometric parameters. Reduced cell spreading area was observed on all three PLLA substrates and a less elongated cell phenotype was seen on PLLA–gAA–gelatin, at high seeding density.

3.3 Extensive intercellular contact masks surface dependence of cell proliferation

When endothelial cells are sparsely-seeded in the sub-confluent state, they are actively proliferating and are sensitive to growth-factor stimulation. Once confluence has been achieved, the cells are contact-inhibited in their growth and protected from apoptosis [31].

Figure 4a shows the cell proliferation profiles on the various PLLA substrates as a function of culture duration, when HUVECs were sparsely seeded at a low density of 5,000 cell/cm^2. Cells grown on TCPS and PLLA–gAA–gelatin proliferated with a doubling time to about 15–16 h. In contrast, cell proliferation showed stagnation on PLLA–gAA–chitosan and even negative on PLLA during the first 72 h, with exponential growth taking place only after 72 h. Figure 4b illustrates the cell proliferation profiles of various PLLA substrates, at a high seeding density of 50,000 cells/cm^2. Cells plated on TCPS, PLLA–gAA–gelatin and PLLA–gAA–chitosan exhibited similar proliferation behavior. Cell proliferation started a few hours after seeding with a doubling time of about 7–9 h during the first 24 h. After 24–72 h, cell proliferation slowed down and eventually stopped. The number of HUVEC on TCPS and PLLA–gAA–gelatin did not increase significantly after 72 h, suggesting that confluence was achieved and that cell–cell contact inhibited proliferation. Cells grown on PLLA displayed an exponential proliferation pattern, which was different from the other three substrates.

Comparing Fig. 4a to Fig. 4b, the profound impact of initial seeding density on cell proliferation is clearly evident. First, low density seeding revealed the superiority of PLLA–gAA–gelatin in supporting cell proliferation compared to PLLA–gAA–chitosan, while extensive intercellular contact at high density seeding masked this difference in EC behavior. Second, by plating a confluent monolayer at high seeding density, the proliferation stagnation on PLLA–gAA–chitosan and PLLA was overcome. In applications involving the in situ endothelialization of cardiovascular implants, such as coronary stents and patent foramen ovale (PFO) occluders, the number of circulating ECs or EC-progenitor cells is relatively low [32]. At high seeding density, PLLA–gAA–gelatin and PLLA–gAA–chitosan showed equivalent performance in cell attachment and proliferation. However, at low seeding density, PLLA–gAA–chitosan showed only marginal improvement in cell

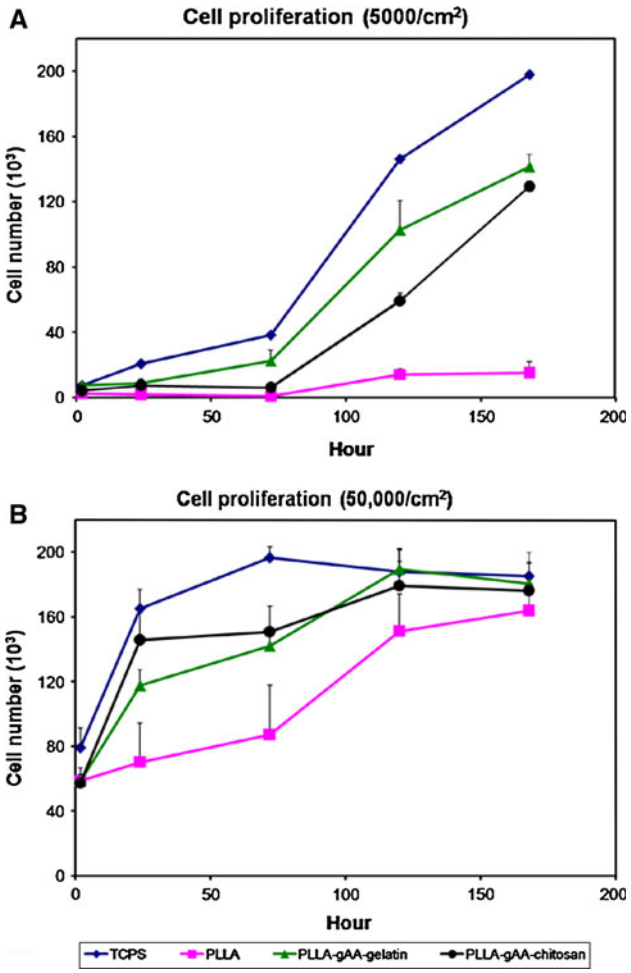

Fig. 4 Extensive intercellular contact masks surface dependence of cell proliferation. Cell proliferation was monitored over 7 days of culture using **(a)** low seeding density of 5,000 cells/cm^2, and **(b)** high seeding density of 50,000 cells/cm^2

attachment and proliferation over PLLA. Clearly, PLLA–gAA–gelatin is a better candidate for such applications, a conclusion that could be reached only through studies at low seeding density.

After confluence was reached, cell morphology was observed through cytoskeletal and focal adhesion immunostaining (Fig. 5). It was found that cell morphology was indistinguishable on the various PLLA surfaces at either low (a, c and e) or high (b, d and f) seeding density. The characteristic cobble-stone morphology was observed with bundles of stress fibers extending from the nucleus to lamellipodia across the entire cytoplasm and terminating at FA and cell–cell junctions (Fig. 5g,h). During cell spreading and proliferation, cells produce their own extracellular matrix with time. The self-synthesized matrix may in turn mask the intrinsic effects of the original substrate on cell proliferation. The results of this study corroborate with earlier reports—that differences in cell

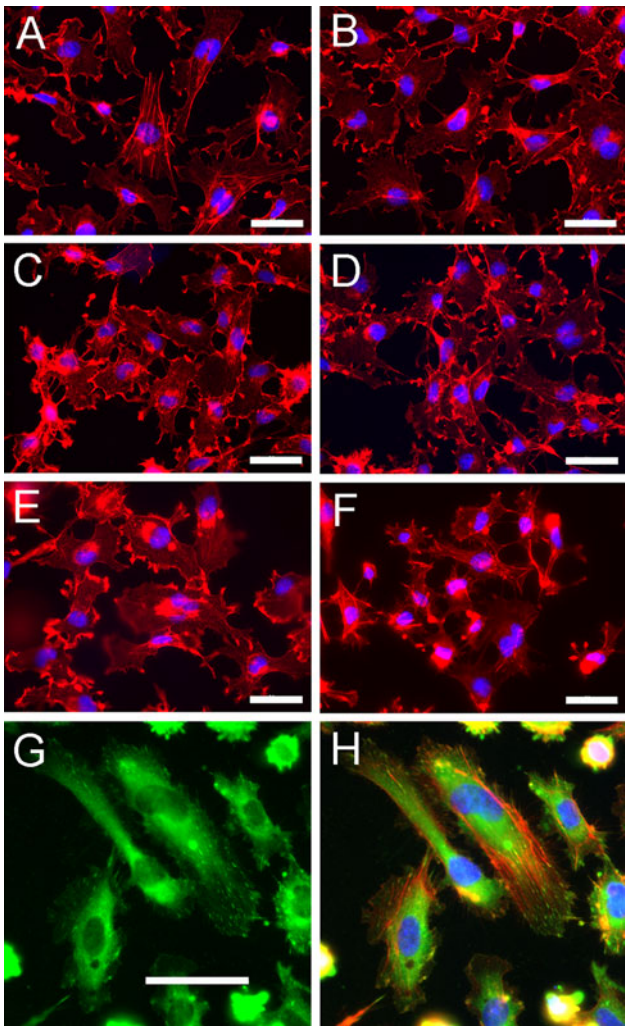

Fig. 5 Substrate dependence of cell morphology disappeared at the point of confluence. Fluorescent micrographs of HUVEC were taken on PLLA (*A* and *B*), PLLA–gAA–gelatin (*C* and *D*), and PLLA–gAA–chitosan (*E* and *F*). Low seeding density of 5,000 cells/cm^2 was used in *A*, *C* and *E*, and high seeding density of 50,000 cells/cm^2 was used in *B*, *D* and *F*. (*G*) Matured FA clusters were observed in HUVEC. (*H*) F-actin bundles terminated at FA clusters by colocalization of F-actin and vinculin. The remaining cells were fluorescently stained to label nuclei (DAPI), vinculin (FITC) and F-actin (Alexa Fluor® 568). The images were captured by Olympus IX71 inverted microscopy. *Scale bar* 50 μm

behavior rising from differences in seeding conditions (substrate and/or density) are more apparent during the first few days of cell–biomaterial interaction [33].

4 Conclusion

This study has demonstrated the important role of seeding density in cell–biomaterial interaction. During the early stage of cell–biomaterial interaction whereby cell attachment is the pre-dominant cellular activity, low seeding density enabled us to observe surface chemistry-dependent cell attachment behavior. Extensive intercellular interactions at high seeding density masked differences amongst substrates, and enhanced cell attachment on all substrates examined. During the later stage of cell-biomaterial interaction, cell proliferation profile was found to be surface-dependent at low seeding density, whereas surface dependence was masked at high seeding density. It is recommended that low seeding density should be utilized for in vitro evaluation the compatibility of biomedical materials.

Acknowledgments Authors would like to thank National Research Foundation of Singapore for funding the work with their Competitive Research Grant and Dr. Wong Yee Shan for critical reading.

References

1. Bhattacharya V, Cleanthis M, Stansby G. Preventing vascular graft failure: Endothelial cell seeding and tissue engineering. Vasc Dis Prev. 2005;2:21–7.
2. Venkatraman SS, Boey F, Lao LL. Implanted cardiovascular polymers: Natural, synthetic and bio-inspired. Prog Polym Sci. 2008;33:853–74.
3. de Mel A, Jell G, Stevens MM, Seifalian AM. Biofunctionalization of biomaterials for accelerated in situ endothelialization: a review. Biomacromolecules. 2008;9:2969–79.
4. Eisenbarth E, Velten D, Breme J. Biomimetic implant coatings. Biomol Eng. 2007;24:27–32.
5. Lu A, Sipehia R. Antithrombotic and fibrinolytic system of human endothelial cells seeded on PTFE: The effects of surface modification of PTFE by ammonia plasma treatment and ECM protein coatings. Biomaterials. 2001;22:1439–46.
6. Yang J, Bei J, Wang S. Enhanced cell affinity of poly (D, L-lactide) by combining plasma treatment with collagen anchorage. Biomaterials. 2002;23:2607–14.
7. Gumpenberger T, Heitz J, Bäuerle D, Kahr H, Graz I, Romanin C, Svorcik V, Leisch F. Adhesion and proliferation of human endothelial cells on photochemically modified polytetrafluoroethylene. Biomaterials. 2003;24:5139–44.
8. Miller DC, Thapa A, Haberstroh KM, Webster TJ. Endothelial and vascular smooth muscle cell function on poly(lactic-co-glycolic acid) with nano-structured surface features. Biomaterials. 2004;25:53–61.
9. Bérard X, Rémy-Zolghadri M, Bourget C, Turner N, Bareille R, Daculsi R, Bordenave L. Capability of human umbilical cord blood progenitor-derived endothelial cells to form an efficient lining on a polyester vascular graft in vitro. Acta Biomater. 2009;5:1147–57.
10. Boura C, Kerdjoudj H, Moby V, Vautier D, Dumas D, Schaaf P, Voegel JC, Stoltz JF, Menu P. Initial adhesion of endothelial cells on polyelectrolyte multilayer films. Bio-Med Mater Eng. 2006;16:S115–21.
11. Chen ZG, Wang PW, Wei B, Mo XM, Cui FZ. Electrospun collagen-chitosan nanofiber: A biomimetic extracellular matrix for endothelial cell and smooth muscle cell. Acta Biomater. 2010;6:372–82.
12. Crombez M, Chevallier P, Gaudreault RC, Petitclerc E, Mantovani D, Laroche G. Improving arterial prosthesis neo-endothelialization: Application of a proactive VEGF construct onto PTFE surfaces. Biomaterials. 2005;26:7402–9.
13. Brewster LP, Bufallino D, Ucuzian A, Greisler HP. Growing a living blood vessel: Insights for the second hundred years. Biomaterials. 2007;28:5028–32.

14. Avci-Adali M, Paul A, Ziemer G, Wendel HP. New strategies for in vivo tissue engineering by mimicry of homing factors for self-endothelialisation of blood contacting materials. Biomaterials. 2008;29:3936–45.
15. Rotmans JI, Heyligers MMJ, Verhagen HJM, Velema E, Nagtegaal MM, de Kleijn DPV, de Groot FG, Stroes ESG, Pasterkamp G. In vivo cell seeding with anti-CD34 antibodies successfully accelerates endothelialization but stimulates intimal hyperplasia in porcine arteriovenous expanded polytetrafluoroethylene grafts. Circulation. 2005;112:12–8.
16. Hill JM, Zalos G, Halcox JPJ, Schenke WH, Waclawiwm MA, Quyyumi AA, Finkel T. Circulating endothelial progenitor cells, vascular function, and cardiovascular risk. N Engl J Med. 2003;348:593–600.
17. Lin A, Ding X, Qiu F, Song X, Fu G, Ji J. In situ endothelialization of intravascular stents coated with an anti-CD34 antibody functionalized heparin-collagen multilayer. Biomaterials. 2010; 31:4017–25.
18. Geiger B, Spatz JP, Bershadsky AD. Environmental sensing through focal adhesions. Nat Rev Mol Cell Biol. 2009;10:21–33.
19. Dejana E. Endothelial cell-cell junctions: happy together. Nat Rev Mol Cell Biol. 2004;5:261–70.
20. Nelson WJ. Regulation of cell–cell adhesion by the cadherin–catenin complex. Biochem Soc Trans. 2008;36:149–55.
21. Arthur WT, Noren NK, Keith B. Regulation of rho family GTPases by cell-cell and cell-matrix adhesion. Biol Res. 2002;35: 239–46.
22. Sakamoto Y, Ogita H, Hirota T, Kawakatsu T, Fukuyama T, Yasumi M, Kanzaki N, Ozaki M, Takai Y. Interaction of integrin $\alpha_v\beta_3$ with nectin: implication in cross-talk between cell-matrix and cell-cell junctions. J Biol Chem. 2006;281:19631–44.
23. Schwartz MA, Ginsberg MH. Networks and crosstalk: Integrin signalling spreads. Nat Cell Biol. 2002;4:E65–8.
24. Geiger B, Bershadsky A, Pankov R, Yamada KM. Transmembrane crosstalk between the extracellular matrix and the cytoskeleton. Nat Rev Mol Cell Biol. 2001;2:793–805.
25. Nagahara S, Matsuda T. Cell-substrate and cell-cell interactions differently regulate cytoskeletal and extracellular matrix protein gene expression. J Biomed Mater Res. 1996;32:677–86.
26. Xia Y, Boey F, Venkatraman SS. Surface modification of poly(L-lactic acid) with biomolecules to promote endothelialization. Biointerphases. 2010;5:FA32–40.
27. Treiser MD, Liu E, Dubin RA, Sung H-J, Kohn J, Moghe P. Profiling cell-biomaterial interactions via cell-based fluorore-porter imaging. BioTechniques. 2007;43:361–8.
28. Zhu Y, Gao C, Liu X, He T, Shen J. Immobilization of biomacromolecules onto aminolyzed poly(L-lactic acid) toward acceleration of endothelium regeneration. Tissue Eng. 2004;10:53–61.
29. Zhu Y, Gao C, Liu Y, Shen J. Endothelial cell functions in vitro cultured on poly(L-lactic acid) membranes modified with different methods. J Biomed Mater Res A. 2004;69A:436–43.
30. Mattila PK, Lappalainen P. Filopodia: molecular architecture and cellular functions. Nat Rev Mol Cell Biol. 2008;9:446–54.
31. Liebner S, Cavallaro U, Dejana E. The multiple languages of endothelial cell-to-cell communication. Arterioscl Throm Vas. 2006;26:1431–8.
32. Huang Y, Venkatraman SS, Boey FYC, Umashankar PR, Mohanty M, Arumugam S. The short-term effect on restenosis and thrombosis of a cobalt-chromium stent eluting two drugs in a porcine coronary artery model. J Interv Cardiol. 2009;22:466–78.
33. Reilly GC, Engler AJ. Intrinsic extracellular matrix properties regulate stem cell differentiation. J Biomech. 2010;43:55–62.